Scientific Research Communications

Research Article

Sci. Res. Comm. (2024)
Volume 4, Issue 1
doi: 10.52460/src.2024.003

Application of Inelastic Nonlinear Buckling Analysis with Stiffness Reduction Factors to Web Tapered I Sections

Oğuzhan Toğay*

[1] Izmir Kâtip Çelebi University, Faculty of Engineering and Architecture, Department of Civil Engineering, İzmir, Türkiye
* Corresponding author: oguzhan.togay@ikcu.edu.tr

Received: 5.01.2024 Accepted: 29.01.2024

Abstract

This paper explores the application of Inelastic Nonlinear Buckling Analysis (INBA) with Stiffness Reduction Factors (SRFs) in the analysis of web-tapered I sections, a structural configuration known for its non-uniform geometry. Leveraging the advanced capabilities of the SABRE2-V2 software, the study investigates the direct load capacity of members and frames, focusing on the implications for structural efficiency and steel material utilization. The inclusion of fixed brace conditions at the midpoint of the beam member, with non-uniform bending, expands the applicability of INBA to complex configurations. The research validates the analytical methods through comparison with Finite Element Analysis (FEA) with four cases that includes different taper angle, achieving an average 98.6% consistency. The study unveils a characteristic S-shaped buckling pattern influenced by strategically placed braces, providing valuable insights into stability and performance optimization. Furthermore, INBA coupled with SRFs elucidates yielding patterns within the member, contributing to a comprehensive understanding of load-carrying behavior and potential failure mechanisms. The findings support the broader adoption of INBA for web-tapered I sections, offering engineers reliable tools for enhanced structural analysis and design. The paper concludes with implications for future research, suggesting exploration of varied taper angles, loading conditions, and material properties.

Keywords: Web-tapered I sections, Inelastic Nonlinear Buckling Analysis (INBA), Stiffness Reduction Factors (SRFs), structural efficiency

1. Introduction

The evolution of structural engineering methodologies has spurred innovative approaches to enhance the analysis and design of steel structures, particularly those with complex geometries. This paper delves into the application of Inelastic Nonlinear Buckling Analysis (INBA) with Stiffness Reduction Factors (SRFs) in the analysis of web tapered I sections—a structural configuration recognized for its non-uniform geometry. The exploration of INBA with SRFs is facilitated through the advanced capabilities of the SABRE2-V2 software, developed by White et al. (2022), offering valuable insights into the direct load capacity of members and frames.

The consideration of web-tapered members holds paramount importance, not only in terms of structural performance but also in terms of the efficient utilization of steel material, positively

impacting economic aspects. Optimizing the use of steel material becomes crucial for achieving structural efficiency, and this paper aims to contribute insights into optimizing the design of web tapered I-sections.

In this topic, Yang and Yau (1987) studied the stability of I beams with tapered webs using differential equations. Andrade et al. (2005) and Boissonnade and Maquoi (2005) showed that prismatic beam elements can be used for the analysis of tapered beams, but without taking into account the bracing strength requirements. Marques et al. (2012), Marques et al. (2013) and Marques et al. (2014) proposed new methods for assessing the resistance of web-tapered columns, beams and beam-columns, based on the Eurocode principles for stability design of members. Recently, Asgarian et al. (2021) presented a theoretical and numerical model based on the power series method for the lateral buckling stability of tapered thin-walled beams with arbitrary cross-sections and boundary conditions. Design Guide 25 (White et al., 2021) provided guidance for the design of web tapered members using different types of braces at various locations and verified the member resistances with hand calculations.

In this study, a distinctive focus is placed on the implementation of fixed brace conditions at the midpoint of the beam member using non-uniform bending. This configuration results in zero moment at one support, gradually increasing linearly towards the other. The utilization of fixed brace conditions introduces a novel dimension to the analysis, broadening the applicability of INBA beyond single-opening members to more complex configurations. This inclusion of bracing applications becomes particularly significant as it expands the scope of INBA, making it applicable not only to conventional members but also to those with intricate geometries and varying support conditions.

While SABRE2-V2, by design, provides direct load capacity information, this study acknowledges the software's limitation in providing detailed post-buckling information. Nonetheless, the software's capacity to simulate inelastic behavior lays the groundwork for a comprehensive exploration of buckling phenomena and initial responses in steel structures.

The literature has highlighted the importance of accurate and reliable analysis methods for predicting the behavior of steel structures with non-uniform geometries. Design Guide (DG25), a document offering suggested methods for the design of web-tapered I-shaped beams and columns, as well as frames incorporating such elements, plays a pivotal role in shaping industry standards. Historical studies by Butler and Anderson (1963) and Prawel et al. (1974) contribute to the understanding of the elastic stability of web and flange tapered beams. Butler and Anderson (1963) focused on investigating the prerequisites for bracing, while Prawel et al. (1974) delved into the topic of inelastic stability, notably considering fixed braces in their experimental analyses.

Building upon this historical and contemporary foundation, White et. al. (2022)'s pioneering work in the development of SABRE2-V2 and its application to INBA with SRFs positions this research at the forefront of advancing the capabilities of structural analysis tools.

As the subsequent sections unfold, this paper will present a detailed theoretical framework of INBA, focusing on the unique application of fixed brace conditions for web tapered I sections. By systematically exploring the effectiveness of this method, considering the non-uniform nature of web tapered I-sections, the research seeks not only to address existing gaps in the literature but also to provide practical insights that can inform the design and assessment of steel structures with enhanced efficiency and structural integrity.

2. Methodology

2.1. Modeling Tapered I Sections with Varying Taper Angles

The paper focuses on assessing the correctness and reliability of the Inelastic Nonlinear Buckling Analysis (INBA) method by investigating the influence of taper angle (α) on the structural behavior of web tapered I sections. Four different values of α—namely, 3, 3.2, 3.4, and 3.6—are considered for the analysis (Figure 1). The modeling of these tapered sections is conducted using two distinct software platforms: ABAQUS Finite Element Software (Simulia, 2020) and SABRE2 (White et. al., 2022).

Figure 1. Test figure of I-tapered web steel sections

2.1.2. Finite Element Analysis (FEA)

The initial aspect of the analysis involves utilizing ABAQUS (Simulia, 2020) to simulate the structural response of the web tapered I sections. The FEA is conducted employing an inelastic nonlinear buckling analysis methodology. The analysis takes into account both residual stresses and geometric imperfections to critically evaluate the correctness of the INBA method under varying taper angles.

2.1.2.1. Residual Stress

The analysis in this study leverages the Best-fit Prawel pattern (Figure 2) within its shell finite element models (FEA) to accurately account for residual stresses. This specific pattern, lauded for its self-equilibrating nature within individual components, has proven effective in past research conducted by Kim (2010) and Subramanian and White (2017). While an alternative approach utilizing half the Best-fit Prawel pattern was considered as suggested from Kim (2010), the full pattern demonstrably exhibited a closer alignment with real-world case studies documented by Smith et al. (2013). Notably, this improved correspondence reinforces the suitability of the Best-fit Prawel pattern (Figure 3) for capturing the intricate residual stress distributions typically encountered in metal building members, as previously investigated by Smith et al. (2013). The preference for the full pattern over the half-pattern further underscores its efficacy in replicating the actual behavior observed in practical engineering scenarios.

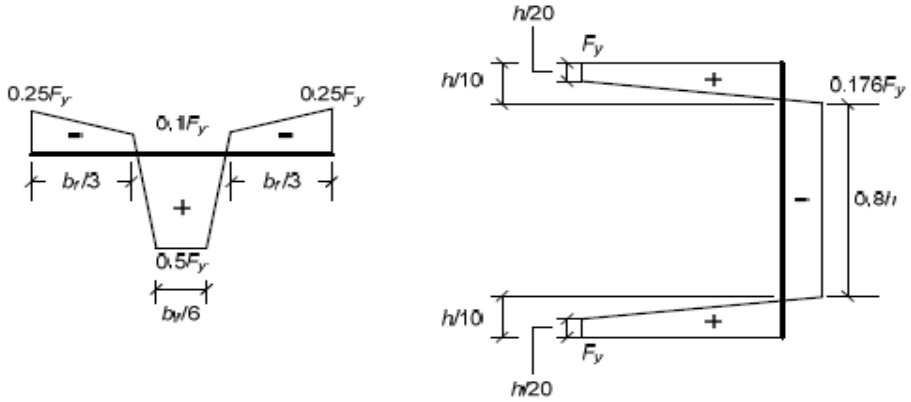

(a) (b)

Figure 2. Best-fit Prawel Pattern (a) flange distribution, (b) web distribution (Adapted from Lokhande, 2014)

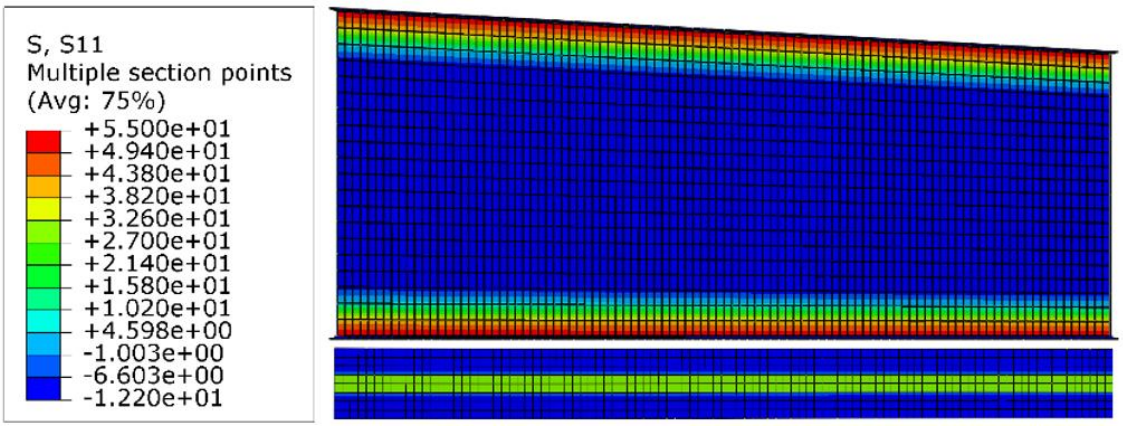

Figure 3. Applied Best-fit Prawel Pattern on α=3.2 case (L_b=127 cm)

2.1.2.2. Geometric Imperfections

To model realistic geometric imperfections in the test simulations, the study adopts half of the tolerance values from the AWS (2010)/AISC Code of Standard Practice (COSP) (2022). This choice is presented by Subramanian and White (2017) demonstrating a strong correlation between these imperfections and experimental data.

To precisely capture web out-of-flatness and flange tilt patterns, the study employs an elastic eigenvalue buckling analysis. This involves subjecting the members to uniform axial compression while strategically restraining out-of-plane displacements at the web-flange juncture points. The resulting buckling modes inform the fine-tuning of flange tilt and web out-of-flatness patterns, ensuring they conform to the specified tolerance values (see Figure 4).

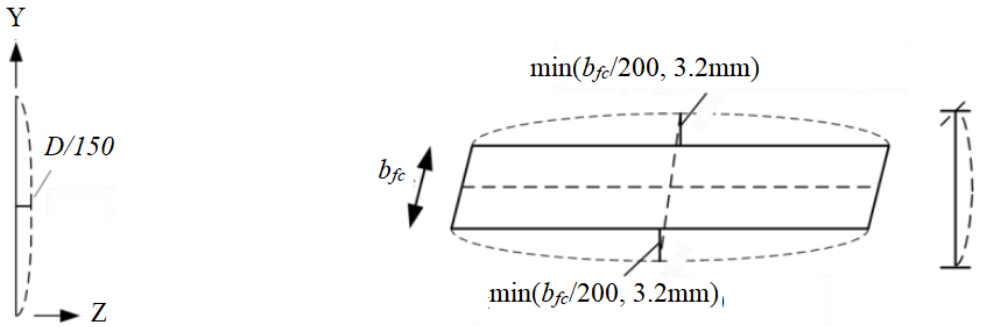

Figure 4. One half of the web out-of-flatness and flange tilt imperfection, adapted from Toğay and White (2017) using Subramanian and White (2017)

Beyond the initial geometric imperfections, the study further complicates the Critical Segment (CS) by introducing a flange sweep at the weld junctions between web and flanges. This sweep, resembling a subtle sinusoidal wave, ripples across the upper flange, which experiences bending under compression. However, the lower flange, subjected to opposite bending forces of tension, remains resolutely straight, devoid of any sweep. This nuanced approach to flange imperfections, captured in Figure 5, adds another layer of complexity to the model, potentially reflecting real-world behavior or serving a specific analytical purpose. The precise details of the sweep's amplitude or wavelength, if relevant, would further illuminate its significance in the study's overall findings.

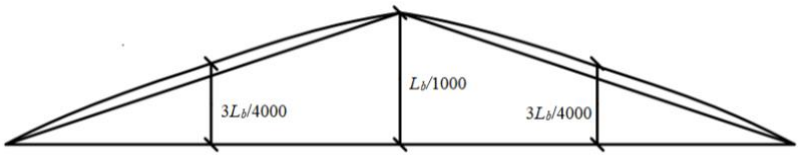

Figure 5. Applied half of the imperfections (the AWS/AISC COSP flange sweep tolerance) on the critical unbraced length, adapted from Toğay and White (2017) using Subramanian and White (2017)

An example model using the above geometric imperfections is presented in Figure 6. The presented figure has α=3.2 and scale factor of 200.

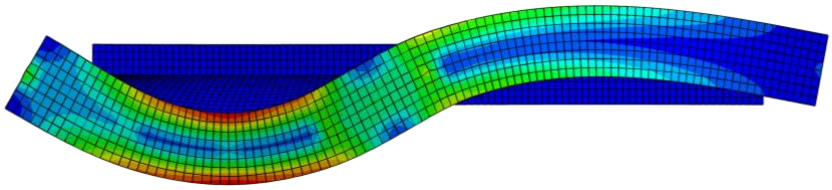

Figure 6. Applied half of imperfections to the finite element model for α=3.2 and scale factor=200 with the S11 stresses plotted

2.1.3. Material Properties

This study utilizes a specific stress-strain curve (Figure 7) to define the steel properties in all test models. The beams are modeled as homogenous materials with a yield strength (F_y) of 379.211 MPa and an elastic modulus (E) of 200 GPa. They behave elastically until reaching a strain of ε_y, followed by a slight increase in hardness until a strain-hardening point at 10 times the yield strain ($10\varepsilon_y$).

Based on the assumed yield strength and the minimum ultimate strength for A572 Grade 55 steel reported by Kim (2010), an ultimate strength (F_u) of 482.632 MPa is further established. Beyond the strain-hardening point, a constant hardening modulus of E/50 is applied, and the material behavior is assumed to be fully plastic, which is not experienced by the members.

It's important to note that the S4R element, which is implemented for the FEA analyses, in ABAQUS software interprets the stress-plastic strain curve logarithmically, which aligns well with the high strains encountered in these simulations. While this approach differs slightly from other true stress-logarithmic strain or engineering stress-strain methods, the discrepancies are minimal. Therefore, the provided stress-strain curve (see Figure 7) offers a reliable approximation of the actual stress-strain behavior of structural steel up to its ultimate strength (F_u).

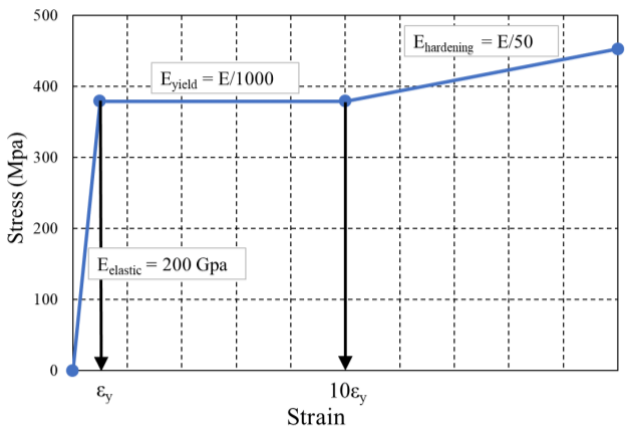

Figure 7. Typical stress-strain curve for Fy = 55 ksi (Kim, 2010)

2.2. FEA Model Validation

This study validates its analytical methods by comparing them to a case study presented in Smith et al. (2013). That study examined the lateral buckling behavior of beam-columns under cyclic loading conditions. Since the current study focuses on the inelastic, nonlinear static response, only the first cycle of the experimental data is analyzed.

Among the ten cases presented by Smith et al. (2013), the CF1 case is chosen for validation (Figure 8). This case features a fixed taper angle, constant flange thickness throughout both top and bottom flanges, and a critical segment within the first unbraced length.

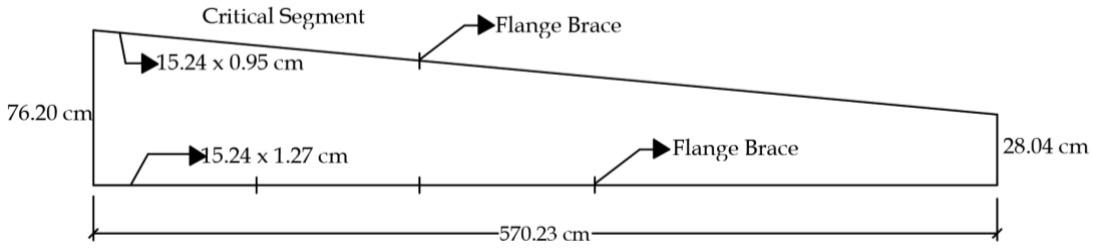

Figure 8. CF1 specimen chosen for the validation study (Smith et. al., 2013)

Figure 9 presents a comparison between the load-deflection curves obtained from the ABAQUS simulations and the actuator load-stiffness data provided by Smith et al. (2013). The values of actuator displacement and force in the simulations are extracted from the support reactions and rotations. From the results of the validation studies, the FEA studies show close correlation with the experimental data.

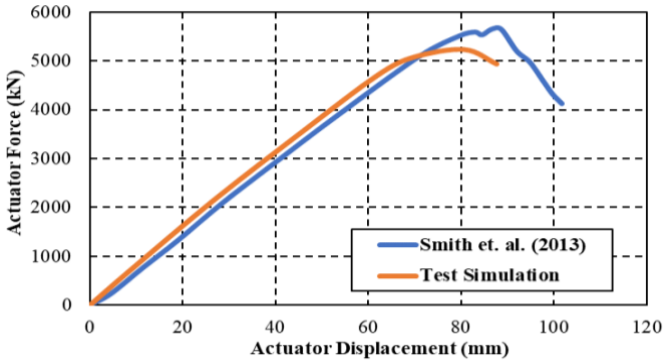

Figure 9. Comparison of test dimulations vs the experimental data of Smith et. al. (2013)

2.3. I-Section Steel Members: A Detailed Examination

The section consists of four steel members, each with a length of 254 centimeters and an unbraced length of 127 centimeters. These members exhibit a web depth of 106.68 centimeters on the left side, featuring a constant thickness of 1.463 centimeters. The taper angles (α) at the top flange location vary from 3 to 3.6 degrees, progressing from the start to the end. The top and bottom flanges maintain a consistent flange width of 22.86 centimeters and a flange thickness of 1.905 centimeters.

The members are supported at both ends, with a fixed top point brace located at the midpoint. The material properties include a yield strength (F_y) of 378.5 MPa for both the web and the top and bottom flanges. The structural model utilizes SABRE2-v2 (White et. al., 2022), as illustrated in Figure 10.

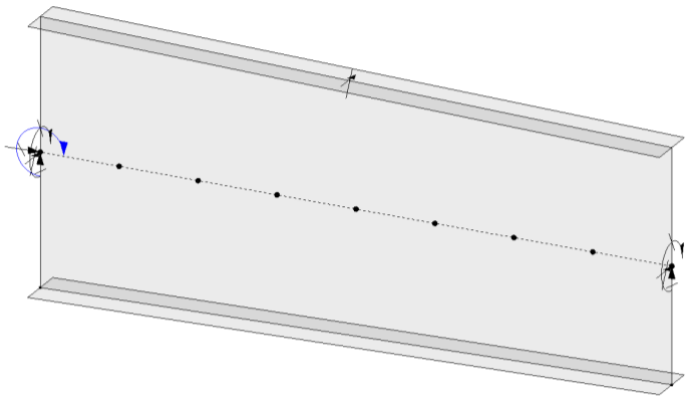

Figure 10. An example model of taper angle 3.0 using SABRE2-V2 (White et. al., 2022)

3. Inelastic Nonlinear Buckling Analysis using Stiffness Reduction Factors

In this section, the stiffness reduction factors (SRFs) for axial, bending, and combined axial and bending loads are given. To keep the paper succinct, only the related equations are given. The derivations of these equations can be found in Toğay (2018).

- Column inelastic stiffness reduction factor, τ_a, is given in Eq. (1) and Eq. (2).
  - For $\left(\frac{\Gamma P_u}{\phi_c P_y} > 0.390\right)$ inelastic buckling controls,

$$\tau_a = -2.724 \frac{\phi_c P_n}{\phi_c P_y} \ln\left(\frac{\phi_c P_n}{\phi_c P_y}\right) \tag{1}$$

  - For $\left(\frac{\Gamma P_u}{\phi_c P_y} \le 0.390\right)$ elastic buckling controls,

$$\tau_a = 1 \tag{2}$$

  where: $\phi_c P_n$: the column factored resistance,

  ΓP_u : internal axial force,

  $\phi_c P_y$: the column factored axial yield strength,

- Beam inelastic stiffness reduction factor, τ_{ltb}, when compact and noncompact web I-section members with $m > \frac{F_L}{F_{yc}}$, where $\phi_b M_{max.LTB} = 0.9 R_b R_{pc} M_{yc}$, is given in Eq. (3).

$$\tau_{ltb} = \sqrt{\frac{Y^4 X^2}{\left[6.76 X^2 \left(\frac{F_{yc}}{E}\right)^2 m^2 + 2Y^2\right]}} \tag{3}$$

where: X and Y are given in Eq. (4) and Eq. (5), respectively.

$$Y = m\left[\frac{\left(1-\frac{m}{R_{pc}}\right)}{\left(1-\frac{F_L}{R_{pc}F_{yc}}\right)}\left(\frac{L_r}{r_t}-\frac{L_p}{r_t}\right)+\frac{L_p}{r_t}\right]\left(\frac{F_{yc}}{E}\right)\left(\frac{1}{1.95}\right) \quad (4)$$

$$X^2 = \frac{S_{xc}h_o}{J} \quad (5)$$

- for slender-web I-sections τ_{ltb} is given in Eq. (6).

$$\tau_{ltb} = \frac{m}{R_b}\left[\frac{\left(R_h - m\frac{1}{R_b}\right)}{\left(R_h-\frac{F_L}{F_{yc}}\right)}\left(\sqrt{\frac{F_{yc}}{F_L}}-\frac{c}{\pi}\right)+\frac{c}{\pi}\right]^2 \quad (6)$$

where: c is 1.1 for the current AISC (2016) Specification and the Stiffness Reduction Factor (SRF) is given in Eq. (7).

$$\text{SRF} = 0.9R_b\tau_{ltb}. \quad (7)$$

4. Results and Discussion

To validate the INBA results presented in Section 2.3, the same members were analyzed using two different software packages: SABRE2-v2 and ABAQUS. SABRE2-v2 utilized an Inelastic Nonlinear Buckling (INBA) approach with Stiffness Reduction Factors (SRFs), while ABAQUS employed Inelastic Nonlinear finite element analysis.

Figure 11 compares the results obtained from both methods, showing the percentage difference between INBA and Finite Element Analysis (FEA) solutions. Notably, the average difference between the two approaches is a mere 1.4%, demonstrating a average 98.6% consistency. This agreement provides strong confidence in the reliability of the INBA results presented earlier.

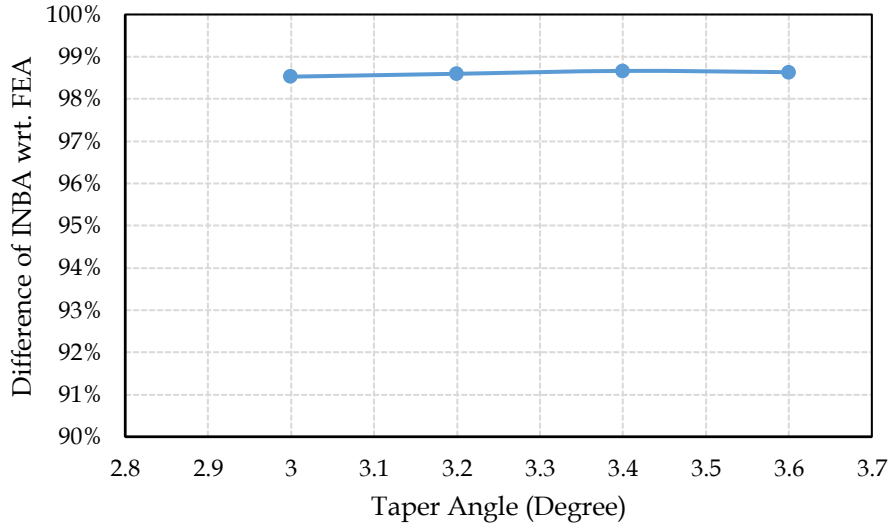

Figure 11. Percentage difference of Inelastic Nonlinear Buckling Analysis (INBA) vs FEA simulations

Figure 12 illustrates the characteristic S-shaped buckled form of a 3.0 taper angle member. Significantly, both the Inelastic Nonlinear Buckling Analysis (INBA) and Finite Element Analysis (FEA) methods yield remarkably similar displaced shapes, underscoring the consistency observed in the quantitative results. This agreement reinforces the validity of the INBA approach for predicting buckling behavior in tapered angle members.

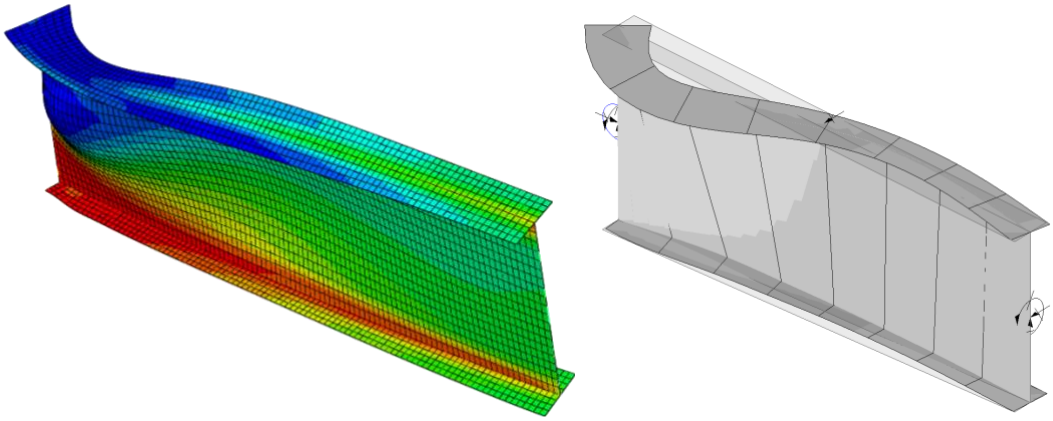

(a) (b)

Figure 12. (a) Finite element analysis buckled shape at the peak load incorporating of S11 stresses, (b) SABRE2-V2 buckled shape at the buckling load proportionality factor (LPF)

The S-shaped buckling pattern is primarily governed by the strategic placement of the brace. By effectively restricting out-of-plane displacement, the brace compels the member to buckle within its own plane, resulting in the distinctive S-shaped configuration.

Beyond predicting buckling behavior, Inelastic Nonlinear Buckling Analysis (INBA) unveils crucial insights into yielding patterns through Stiffness Reduction Factors (SRFs). These factors quantify the extent of yielding within structural sections, acting as indispensable indicators of a member's overall capacity to resist deformation.

The SRF plot generated for the tapered angle member in SABRE2-v2 paints a vivid portrait of yielding distribution (Figure 13). It reveals a striking gradient of SRF values, commencing at a minimum of 0.147 on the left side and culminating in a maximum of 1.0 on the right side. This gradient conveys several key interpretations:

- Yielding Localization: The low SRF value of 0.147 on the left side signals substantial yielding within that region, indicating a concentration of plastic deformation. This localization likely stems from a combination of factors, including geometric variations, stress concentrations, or material inhomogeneities.

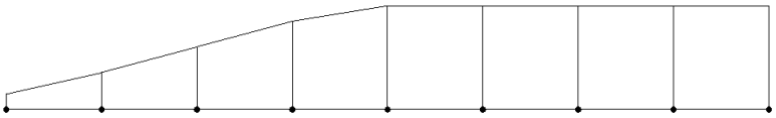

Figure 13. SRF plot of taper angle of 3.0

- Unyielded Region: Conversely, the SRF value of 1.0 on the right side signifies a complete absence of yielding, implying the material in that region remains within its elastic range. This disparity in yielding patterns highlights the complex interplay between member geometry, loading conditions, and material properties.
- Yield Progression: The gradual increase in SRF values from left to right suggests a progressive transition from a highly yielded state to an unyielded state along the member's length. This pattern offers valuable insights into the member's load-carrying behavior and potential failure mechanisms. The PEEQ contour of the member with a

taper angle of 3.0 exhibits a close correlation with the SRF plot (Figure 14). Non-zero PEEQ values are colored red, indicating the spread of yielding at the peak load proportional factor, while zero PEEQ values are blue, illustrating where the plates remain elastic. This observation enhances the understanding of the specific behavior of the tapered member under load, providing a comprehensive view of its structural response and failure characteristics.

- Safety Factor Considerations: While a safety factor of 0.9 is typically applied in design practice to account for uncertainties, its omission in this analysis facilitates a direct comparison with Finite Element Analysis (FEA) results, ensuring a consistent basis for validation.

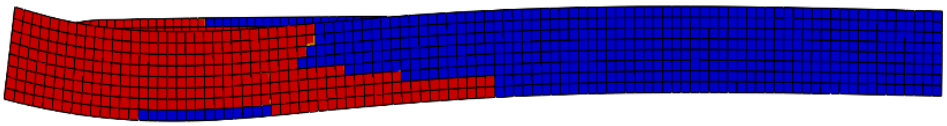

Figure 14. PEEQ contours on the deformed geometry from the top view (scale factor: 1)

5. Conclusions

This research has systematically investigated the application of Inelastic Nonlinear Buckling Analysis (INBA) with Stiffness Reduction Factors (SRFs) to web tapered I sections, a growing trend in modern steel design. The findings provide valuable insights into the buckling behavior of these complex elements, paving the way for optimized design and analysis techniques.

The significant agreement between INBA and Finite Element Analysis (FEA) results, with a remarkable 98.6% consistency, validates the accuracy and robustness of INBA for assessing the buckling response of web tapered I sections, particularly those with fixed brace configurations. This validation paves the way for the broader adoption of INBA in this domain, enhancing the reliability and efficiency of structural analysis for these increasingly popular elements.

Furthermore, the analysis revealed the characteristic S-shaped buckling pattern observed in the test member, a direct consequence of the strategically placed fixed brace. This observation highlights the effectiveness of the brace in mitigating out-of-plane deformations, offering valuable guidance for engineers seeking to optimize the stability and performance of web tapered I sections in their designs.

Beyond predicting buckling behavior, INBA coupled with SRFs provides crucial insights into the internal distribution of yielding within the member. The gradient of SRF values, indicative of concentrated plastic deformation on one side and an unyielded region on the other, illuminates the member's load-carrying capacity and potential failure mechanisms. This knowledge empowers engineers to design more robust and resilient structures, maximizing the efficiency and lifespan of web tapered I sections.

While this research has made significant strides in understanding the nuances of web-tapered I sections, it also acknowledges the need for further investigation. Future research could explore the influence of various taper angles, loading conditions, and material properties on their buckling behavior and yielding patterns. Additionally, analyzing the response of these elements under dynamic or cyclic loading could offer valuable insights for practical applications.

Author Statement

The author confirms sole responsibility for the following: study conception and design, data collection, analysis and interpretation of results, and manuscript preparation.

Conflict of Interest

The authors declare no conflict of interest.

References

AISC (2016). Specification for Structural Steel Building. *American Institute of Steel Construction.*

AISC (2022). Specification for Structural Steel Building. *American Institute of Steel Construction.*

AWS (2010). Structural Welding Code–Steel, *AWS D1.1: D1.1M*, (22nd ed.), prepared by AWS Committee on Structural Welding, 572.

Andrade, A., Camotim, D., & e Costa, P.P. (2005). Elastic Lateral-Torsional Buckling Behavior of Doubly Symmetric Tapered Beam-Columns Proceedings. *Annual Stability Conference*, *Structural Stability Research Council*, Montreal, Quebec, Canada, 445-468

Asgarian, B., Soltani, M., & Mohri, F. (2013). Lateral-torsional Buckling of Tapered Thin-Walled Beams with Arbitrary Cross-sections. *Thin-Walled Structures*, 62, 96-108,

Boissonnade, N., & Maquoi, R. (2005). A Geometrically and Materially Non-linear 3-D Beam Finite Element for the Analysis of Tapered Steel Members, *Steel Structures*, 5, 413-419.

Butler, D. J., & Anderson G. C. (1963). The Elastic Buckling of Tapered Beam-Columns. *Welding Journal Research Supplement*.

Kim, Y. D. (2010). Behavior and Design of Metal Building Frames with General Prismatic and Web-Tapered Steel I-Section Members. *Doctoral Dissertation*. School of Civil and Environmental Engineering, Georgia Institute of Technology, Atlanta, GA, 562 pp. n.d.

Lokhande, A. M. (2014). Evaluation Of Steel I-Section Beam And Beam-Column Bracing Requirements By Test Simulation, *Master Thesis*, School of Civil and Environmental Engineering, Georgia Institute of Technology, Atlanta, GA.

Marques, L., Taras, A., Simões da Silva, L., Greiner, R., & Rebelo, C. (2012). Development of a Consistent Buckling Design Procedure for Tapered Columns. *Journal of Constructional Steel Research*, 72, 61-74.

Marques, L., Simões da Silva, L., Greiner, R., Rebelo, C. and Taras, A. (2013). Development of a Consistent Design Procedure for Lateral–Torsional Buckling of Tapered Beams. *Journal of Constructional Steel Research*, 89, 213-235.

Marques, L., Simões da Silva, L., Rebelo, C., & Santiago, A. (2014). *Extension of EC3-1-1 Interaction Formulae for the Stability Verification of Tapered Beam-Columns*, 100, 122-135

Prawel, S. P., Morrell M. L., & Lee G. C. (1974). Bending and Buckling Strength of Tapered Structural Members, *Welding Research Supplement*, 53, 75-84.

Simulia. (2020). ABAQUS , Version 6.20. *Software and Analysis User's Manual*.

Smith, M. D., Turner, K. A., & Uang, C. M. (2013). Experimental Study of Cyclic Lateral-Torsional Buckling of Web-Tapered I-Beams. Report No. SSRP-12/06, *Final Report to Metal Building Manufacturers Association*, Department of Structural Engineering, Univ.

Subramanian, L., & White, D. W. (2017). Resolving the Disconnect between Lateral Torsional Buckling Experimental Tests, Test Simulations and Design Strength Equations. *Journal of Constructional Steel Research*, 128, 321-334.

Toğay, O. (2018). Advanced Design Evaluation Of Planar Steel Frames Composed Of General Nonprismatic I-Section Members. *Doctoral Dissertation*, School of Civil and Environmental Engineering, Georgia Institute of Technology, Atlanta, GA, 273 pp.

Toğay, O., & White, D. W. (2017). Comprehensive Stability Design of Steel Members and Systems via Inelastic Buckling Analysis–Beam-Column Validation Studies. *Proceedings of the Annual Stability Conference Structural Stability Research Council*. San An.

White, D. W., Jeong, W. Y. & Slein, R. (2021). Frame Design Using Nonprismatic Members, *AISC/MBMA Design Guide 25,* 2nd Ed., American Institute of Steel Construction, Chicago, IL, 405

White, D. W., Toğay, O. W., Jeong, Y., & Slein, R. (2022). *SABRE2-V2.* white.ce.gatech.edu/sabre.

Yang, Y. B., & Yau, J. D. (1987). Stability of Beams with Tapered I-Sections. *ASCE J. Eng. Mech.*, 113 (9), 1337–1357.